

2011 Symposium on Human Body Dynamics

# Simulation and design of an active orthosis for an incomplete spinal cord injured subject

Josep M. Font-Llagunes<sup>a,\*</sup>, Rosa Pàmies-Vilà<sup>a</sup>, Javier Alonso<sup>b</sup>, Urbano Lugrís<sup>c</sup>

<sup>a</sup>*Department of Mechanical Engineering and Biomedical Engineering Research Centre, Universitat Politècnica de Catalunya, Diagonal 647, 08028 Barcelona, Spain*

<sup>b</sup>*Department of Mechanical Engineering, Universidad de Extremadura, Avda. de Elvas s/n, 06006 Badajoz, Spain*

<sup>c</sup>*Laboratory of Mechanical Engineering, Universidad de La Coruña, Mendizábal s/n, 15403 Ferrol, Spain*

---

## Abstract

The dynamic simulation of incomplete spinal cord injured individuals equipped with active orthoses is a challenging problem due to the redundancy of the simultaneous human-orthosis actuation. The objective of this work is two-fold. Firstly, a physiological static optimization approach to solve the muscle-orthosis actuation sharing problem is presented. For this purpose, a biomechanical model based on multibody dynamics techniques is used. The muscles are modeled as Hill-type actuators and the atrophy of denervated muscles is considered by adding stiff and dissipative elements. Secondly, the mechanical design of a new active stance-control knee-ankle-foot orthosis (A-SCKAFO) is addressed. The proposed device consists of a passive joint that constrains ankle plantar flexion, along with a powered knee unit that prevents flexion during stance and controls flexion-extension during swing. The knee actuation is selected based on the results obtained through the optimization approach.

© 2011 Published by Elsevier Ltd. Open access under [CC BY-NC-ND license](https://creativecommons.org/licenses/by-nc-nd/4.0/).

Peer-review under responsibility of John McPhee and József Kövecses

*Keywords:* Active orthosis; Biomechanics; Static optimization; Muscle modeling

---

## 1. Introduction

Spinal cord injuries (SCI) cause paralysis of the lower limbs as they break the connections from the nervous central system to the muscular units of the lower body. There are different SCI levels according to the standard neurological classification of SCI of the American Spinal Injury Association (ASIA).

---

\* Corresponding author. Tel.: +34 93 4054113; fax: +34 93 4015813.

E-mail address: [josep.m.font@upc.edu](mailto:josep.m.font@upc.edu).

Those are classified by the ASIA Impairment Scale (AIS) and range from A (complete SCI) to E (normal motor and sensory function). The presented active orthosis is aimed at assisting incomplete SCI subjects with AIS level C or D. In these cases, the motor function in the key lower limb muscle groups is partially preserved, and patients can perform a low-speed, high-cost pathological gait by using walking aids such as crutches, canes or parallel bars. The energy cost and aesthetics of this walk can be improved by means of active orthoses [1,2], which require external actuation mechanisms to control the motion of the leg joints during the different phases of human gait.

The first controllable active orthosis was developed in 1942. It was a hydraulically actuated device to assist the hip and knee joints [3]. The first exoskeletons to assist paraplegic subjects were developed in the seventies [4], but had little success because they were limited to predefined joint motions. Nowadays, orthotic systems use predefined patterns of joint motions and torques together with classical control techniques or EMG-based control, with the aim of integrating the human musculoskeletal system and the assistive device [5].

Orthoses can generally be classified according to the joint for which they are designed [6]. The function of an ankle-foot-orthosis (AFO) is to guide ankle plantar and dorsiflexion. In some cases, such as cerebral palsy or SCI, the AFO is used to avoid excessive plantar flexion which is one of the causes of drop-foot gait [7]. The knee-ankle-foot-orthosis (KAFO) is used by patients with more severe gait dysfunctions, including partial or complete paralysis of the lower limbs [8]. One particular type of KAFO is the stance-control knee-ankle-foot-orthosis (SCKAFO), which is well-suited for patients with incomplete SCI [1,9]. This device permits free knee motion during swing and locks knee flexion during stance. There are also hip-knee-ankle-foot-orthoses (HKAFO) that assist all lower limb joints [6].

These devices can be passive mechanisms that support weakened or paralyzed body segments, or active devices including actuation to assist joint motion using an external power source. Blaya and Herr [10] developed an active AFO to assist drop-foot gait. This is based on a linear series elastic actuator to assist ankle motion and it uses plantar sensors and potentiometers to detect the phases of gait. Similar designs have been presented for rehabilitation of SCI [11], or for knee motion assistance in healthy subjects to reduce the metabolic cost of locomotion [12]. Kawamoto and Sankai [13] developed the HAL (Hybrid Assistive Limb), an exoskeleton actuated by rotary motors, which is designed to assist the lower limbs of elderly people. Its control system generates external joint torques based on EMG measurements, foot-ground contact forces and joint angles. Pneumatic artificial muscles (McKibben muscles) are also used in AFO and KAFO as shown in [14,15]. The KAFO presented in [14] consists of 6 artificial muscles (2 at the ankle joint and 4 at the knee joint) that mimic the agonist-antagonist pairs of the human body.

In the first part of the paper, we present an algorithm to quantify the simultaneous contributions of muscles and orthosis to the net joint torques of the human-orthosis system. This is a useful tool to assist the selection of external actuators in the design of active orthotic devices. In the presented approach, the net joint torques are first obtained through an inverse dynamics analysis using a multibody biomechanical model and kinematic data of normal walking. Then, passive joint torques are added in order to account for muscle atrophy in spinal cord injured subjects. The stiffness and damping parameters to quantify the passive torques are obtained from the literature. Finally, the muscle-orthosis redundant actuator problem is solved through a physiological static optimization approach with a cost function that accounts for muscular and robotic energy consumption. Muscles are modeled as Hill-type actuators, and a weakness factor is used to limit muscle activation in partially functional muscles. In this approach, the “generic” orthosis is included as a set of external torques added to the anatomical joints so as to obtain net joint torque patterns similar to those of normal unassisted walking. The hypothesis that subjects walk with similar net joint torque patterns (rather than kinematic patterns) when walking with and without robotic external assistance is supported by Kao et al. [15].

In the second part, we present a new design of an active stance-control knee-ankle-foot-orthosis (A-

SCKAFO) to assist incomplete spinal cord injured subjects with AIS level C or D. This is intended for SCI that preserves normal motor function of the hip flexors and extensors, but presents partially denervated muscles at the knee and ankle joints. The results of simulations using the previous physiological optimization approach are used to select the proper knee actuation during swing phase. The detailed mechanical design of the developed assistive device is presented. The knee unit actuates the knee flexion-extension during swing and locks the knee flexion during stance by means of a commercial controllable locking system. The ankle unit includes a passive joint that applies an external torque so as to avoid drop-foot gait and limits ankle dorsiflexion. Both units are modular and can be easily adapted to standard orthoses. The orthosis is equipped with the required sensors for its autonomous operation.

## 2. Musculoskeletal modeling

This section presents the biomechanical multibody model used to obtain the net joint torques for normal walking and the muscle models for the functional (innervated) and partially denervated muscles of the spinal cord injured subject.

### 2.1. Biomechanical multibody model

The biomechanical model used has 14 degrees of freedom. It consists of twelve rigid bodies linked with revolute joints and it is constrained to move in the sagittal plane, Fig. 1a. Each rigid body is characterized by mass, length, moment of inertia about the center of mass, and distance from the center of mass to the proximal joint. In order to quantify the simultaneous contributions of the musculoskeletal system and a generic active orthosis to the net joint torques of the human-orthosis system, eight muscle groups and three external torques added to the lower limb joints,  $T_{o,1}$ ,  $T_{o,2}$  and  $T_{o,3}$ , were considered in this analysis, Fig. 1b.

The equations of motion of the biomechanical multibody system can be written as

$$\mathbf{M}\ddot{\mathbf{q}} + \Phi_{\mathbf{q}}^T \boldsymbol{\lambda} = \mathbf{Q}, \quad (1)$$

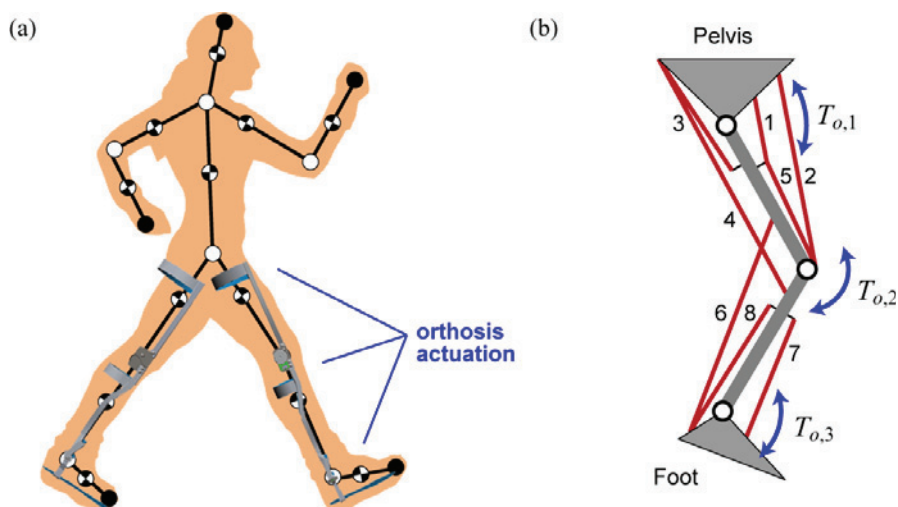


Fig. 1. (a) Biomechanical model of the human-orthosis system; (b) Muscle groups of the lower limb: 1 – Iliopsoas, 2 – Rectus Femoris, 3 – Glutei, 4 – Hamstrings, 5 – Vasti, 6 – Gastrocnemius, 7 – Tibialis Anterior, 8 – Soleus.

where  $\mathbf{M}$  is the mass matrix of the system,  $\Phi_{\mathbf{q}}$  is the Jacobian matrix of the constraint equations,  $\ddot{\mathbf{q}}$  is the acceleration vector,  $\mathbf{Q}$  is the generalized force vector and  $\lambda$  are the Lagrange multipliers. Using kinematic and anthropometric data, the net joint torques during a physical activity or motion and the resultant force and moment due to body-ground contact can be calculated through Eq. (1). The input data corresponds to the 2D walking kinematic benchmark from Winter [16].

## 2.2. Muscle modeling: Innervated and denervated muscles

Injury to the human spinal cord typically results in complete or partial paralysis of muscles innervated by spinal segments at or below the trauma. The degree of denervation depends on the severity of the SCI. The AIS (ASIA Impairment Scale) level indicates the severity of the injury from A (complete) to E (normal motor and sensory functions). In the C and D levels, the motor function is preserved below the neurological level (lowest segment where motor and sensory functions are normal), being the difference between C and D the muscle activity grade of the key muscular groups. The muscle activity grade ranges from 0 (total paralysis) to 5 (active movement, full range of motion, normal resistance). In this work, the weakness of denervated muscles is modeled through a *weakness factor*  $p \in [0,1]$  that limits the maximum activation of those muscles.

Both innervated (functional) and partially denervated muscles are modeled as Hill-type actuators. The Hill-type muscle-tendon model [17,18], which is shown in Fig. 2, consists of a contractile element (CE) that generates the force, a nonlinear parallel elastic element (PE), representing the stiffness of the structures in parallel with muscle fibers, and a nonlinear series elastic element (SE) that represents the stiffness of the tendon which is serially attached to the muscle and completes the muscle-tendon unit.

The two differential equations that govern the muscle dynamics are

$$\dot{a} = h(u, a), \quad (2)$$

$$\dot{f}_{mt} = g(a, f_{mt}, l_{mt}, v_{mt}). \quad (3)$$

The first equation is the activation dynamics equation that relates muscle excitation  $u$  from the central nervous system and muscle activation  $a \in [0,1]$ . Eq. (3) defines the force-generation properties as a function of the muscle-tendon length  $l_{mt}$  and velocity  $v_{mt}$ . In order to account for muscle weakness, the muscle activation will be multiplied by the above mentioned weakness factor  $p$ ; where  $p=1$  for innervated muscles,  $0 < p < 1$  for partially denervated muscles, and  $p=0$  for completely paralyzed muscles. In this work the activation dynamics is not considered.

The force generated by the CE,  $f_{ce}$ , is function of the activation  $a$ , the CE length  $l_{ce}$ , and its contraction velocity  $v_{ce}$ . For a detailed description of these relationships the reader is referred to [19]. If the pennation angle  $\alpha$  is constant, then according to Fig. 2b

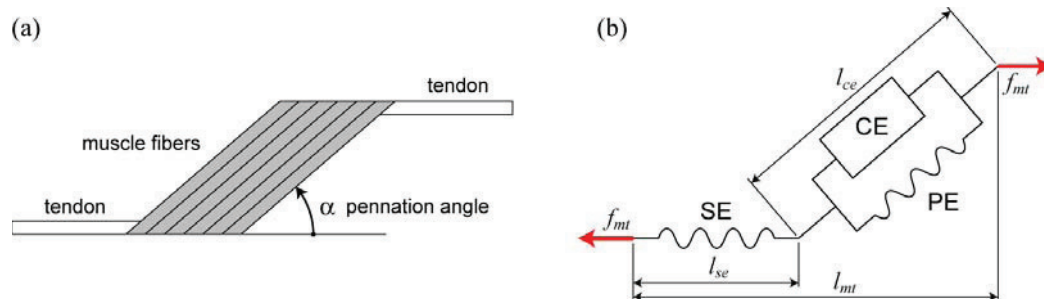


Fig. 2. Muscle model: (a) Conceptual scheme; (b) Hill model [17].

$$l_{mt} = l_{se} + l_{ce} \cos \alpha, \quad (4)$$

$$f_{mt} = f_{se} = (f_{ce} + f_{pe}) \cos \alpha \approx f_{ce} \cos \alpha, \quad (5)$$

where the force of the parallel elastic element PE is set to zero [19–21]. The tendon (SE) can be modeled by a simple quadratic force-strain curve depending on the tendon stiffness. All the values of healthy muscle parameters are obtained from [19].

Apart from the decrease in the amount of maximum activation, partially functional muscles show features of denervation atrophy [22], whose severity depends on the time elapsed from the injury. The atrophy of denervated muscles increases the passive torques at the joints, which include the torques generated by all other passive structures crossing the joints (e.g., ligaments, etc.). Several studies show that passive torques tend to be larger in pathological than in healthy individuals [23,24]. To model the increment of passive torque due to muscle atrophy, stiff and dissipative elements have been added to joints. A linear damping and nonlinear stiffness, which were estimated from experimental data of SCI subjects, have been added to the knee and ankle joints. Their values are the approximate average values obtained from pendulum experiments [23,24].

The calculation of the passive torque due to muscle atrophy is important to determine the torque needs of the active orthotic device to assist gait. Fig. 3 shows the increment of the ankle and knee torques due to pathological passive torque compared with the torques in normal gait (obtained through inverse dynamics analysis from the 2D walking kinematic benchmark from Winter [16]). The results show very slight differences except for the knee flexion-extension during the swing phase (from 0 to 0.40 in normalized time). No additional passive torque has been added to the hip joint because hip muscles are assumed to be fully innervated in the considered incomplete SCI subjects (AIS levels C and D).

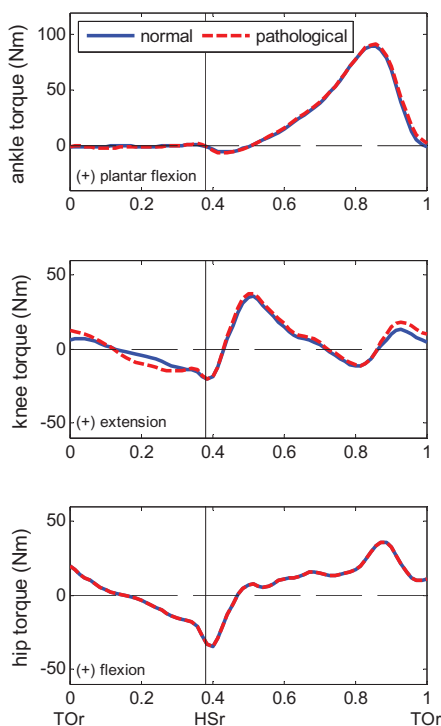


Fig. 3. Ankle, knee and hip torques during normal gait (solid blue line) and pathological gait (dashed red line) in normalized time scale. TOr: right toe off; HSr: right heel strike. The vertical continuous line separates the swing and stance phases of gait.

### 3. Solution to the simultaneous muscle-orthosis actuation

Since several muscles serve each joint of the skeletal system, muscle forces cannot be directly computed from joint torques. This is the well-known load sharing problem in biomechanics. In order to solve this problem, optimization procedures are used. Several optimization methods (static optimization, dynamic optimization, augmented static optimization, large-scale static optimization) and optimization criteria (minimum metabolic cost of transport, minimum sum of muscle stresses, minimum sum of muscle activations, etc.) are available in the literature [25-30]. The optimization assumes that the load sharing between the muscles follows certain rules during learned motor activities and muscle recruitment strategy is governed by physiologic criteria that achieve functional efficiency. In our problem, musculoskeletal forces are complemented by the orthosis external torques resulting in a more complex problem that involve both muscle and orthosis actuation.

#### 3.1. Physiological static optimization approach

A modified version of the classical static optimization approach is proposed in this section to solve the force sharing problem at the lower limb joints [31]. This scheme considers the muscle contraction dynamics ensuring the physiological consistency of the obtained solution. The proposed optimization approach comprises two steps. In the first step, the inverse contraction dynamics problem is solved, assuming that muscle activations are maxima. The length and velocity of each muscle-tendon unit  $l_{mt}$ ,  $v_{mt}$  are calculated from the mechanical state of the multibody system. Then, the maximum muscle force histories  $\mathbf{F}_{mt}^*$  compatible with contraction dynamics are calculated assuming that the muscle activations are maxima at each instant  $\mathbf{A}_m \equiv [a_1, \dots, a_N]^T = [p_1, \dots, p_N]^T$ , where  $N = 8$  is the number of muscle groups considered, see Fig. 1b. Briefly, for each muscle, the contraction dynamics differential equation is integrated

$$\frac{df_{mt}^*}{dt} = g(a = p, f_{mt}, l_{mt}, v_{mt}). \quad (6)$$

In the second step, the muscle activations and orthosis actuation are calculated solving the following static optimization problem at each time step

$$\begin{aligned} \text{Min} \quad & J(\mathbf{A}_m, \mathbf{A}_o) = \omega_m \sum_{j=1}^N \left( -a_j f_{mt,j}^* v_{mt,j} \right)^2 + \omega_o \sum_{k=1}^3 \left( a_{o,k} T_{o,k}^* \dot{\theta}_k \right)^2, \\ \text{s.t.} \quad & \mathbf{R}(\mathbf{A}\mathbf{F}^*) = \mathbf{T}, \\ & 0 \leq a_j \leq 1, \quad j = 1, \dots, N = 8, \\ & -1 \leq a_{o,k} \leq 1, \quad k = 1, 2, 3, \end{aligned} \quad (7)$$

where the objective function  $J$  is the weighted sum of the squared muscle power and the squared orthosis actuation power,  $\omega_m$  and  $\omega_o$  are the weights related to muscle and orthosis actuation,  $T_{o,k}^*$  are the maximum torques that the orthosis can exert,  $\dot{\theta}_k$  are the joint angular velocities ( $k = 1$  for the hip,  $k = 2$  for the knee, and  $k = 3$  for the ankle),  $\mathbf{A}$  is the combined muscle-orthosis activation matrix,  $\mathbf{A}\mathbf{F}^* = [a_1 f_{mt,1}^*, \dots, a_N f_{mt,N}^*, a_{o,1} T_{o,1}^*, \dots, a_{o,3} T_{o,3}^*]^T$  is the muscular and orthosis actuation vector,  $\mathbf{R}$  is the matrix of equivalent moment arms of the different muscle groups and orthosis actuators, and  $\mathbf{T}$  is the vector of net joint torques obtained from inverse dynamics analysis (considering the dissipative effects of denervated muscles). Moment arms are defined as the distance between the muscle line of action and the

joint axis of rotation. The muscle lengths and moment arms can be determined as functions of the generalized coordinates using expressions or tables available in the literature (see, for example, [30]). The first constraint imposes that the total contributions of muscles and orthosis actuators has to equal the torques obtained from the inverse dynamics analysis, see Fig. 3. The second and third constraints impose that muscular forces and orthosis torques lie within their limits.

### 3.2. Simulation results and discussion

As mentioned before, normal gait motion data is used as input to the inverse dynamics analysis. The acquired motion is a normal cadence non-pathological gait stride, carried out by a healthy female subject with 57.75 kg of weight. The kinematic data are acquired using a sampling frequency of 70 Hz. Once the joint torques in Fig. 3 are obtained, the optimization problem is solved using the MATLAB gradient-based routine *fmincon* implemented in the optimization toolbox that uses a sequential quadratic programming (SQP) method.

We have simulated the muscle-orthosis actuation for two cases of SCI, a subject with incomplete SCI with AIS level C and another with AIS level D. In both AIS levels C and D, the motor function is preserved below the neurological level. The difference between those levels is the number of key muscles below the neurological level that have a muscle activity grade less than 3. In AIS level C, more than half of key muscles below the neurological level have a muscle grade less than 3. In AIS level D, at least half of key muscles below the neurological level have a muscle grade of 3 or more. Thus, we have defined the following vectors of weakness factors to simulate both subjects:

- AIS C subject:  $\mathbf{p} = [1, 0.2, 1, 0.2, 0.2, 0.2, 0.2, 0.2]^T$ .
- AIS D subject:  $\mathbf{p} = [1, 0.6, 1, 0.6, 0.6, 0.4, 0.4, 0.4]^T$ .

Note that in both cases the hip monoarticular muscles (iliopsoas and glutei) are assumed fully innervated. We have simulated the actuation provided by a generic active knee-ankle-foot orthosis (A-KAFO) in order to obtain a combined torque pattern as in unassisted normal walking. In the present example, the hip is not externally actuated and, therefore, the maximum available orthosis torque at the hip is assumed  $T_{o,1}^* = 0$ .

Results show that a proper A-KAFO can assist the pathological gait cycle of incomplete SCI subjects with AIS levels C and D to obtain kinetic gait patterns similar to normal walking. Figs. 4 and 5 show the ankle and knee joint torques and the forces exerted by the eight muscle groups, respectively. Those are the outputs obtained from the optimization approach. It can be observed that the orthosis actuation prevents stance phase knee flexion (extension moment) due to quadriceps weakness, assists swing-phase knee flexion-extension and corrects insufficient ankle plantar flexor torque to achieve normal torque patterns along the gait cycle, Fig. 4.

The results clearly show that the AIS C subject requires more external actuation than the AIS D subject in order to achieve a normal torque pattern. This difference is more significant in the ankle torque rather than in the knee. During the gait cycle the muscle groups of the AIS D subject exert more force than the ones of the AIS C subject, Fig. 5. Particularly, the rectus femoris, the gastrocnemius and the soleus are the muscles that experience more difference in activation levels for the two simulated SCI subjects.

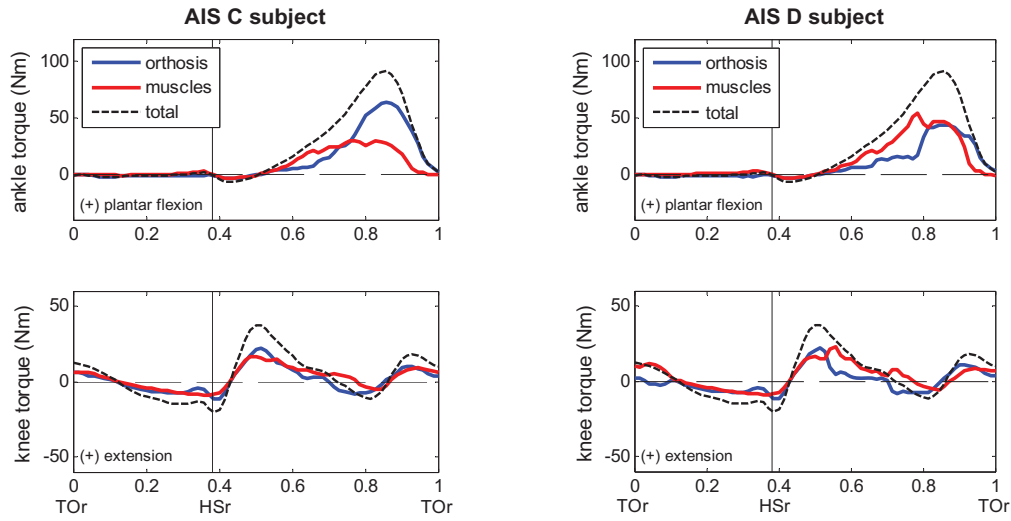


Fig. 4. Knee and ankle torques exerted by muscles and orthosis for the SCI subjects with AIS level C (left) and AIS level D (right) in normalized time scale. TOr: right toe off; HSr: right heel strike. The vertical continuous line separates the swing and stance phases of gait.

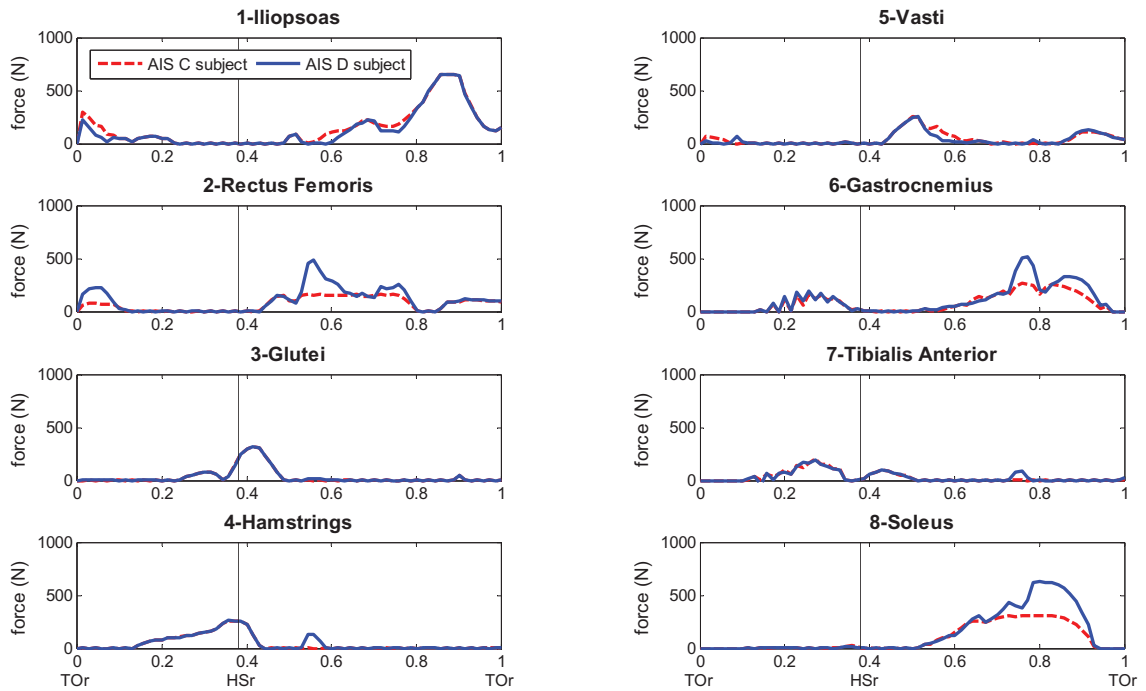


Fig. 5. Muscle forces for the SCI subjects with AIS level C (dashed red line) and AIS level D (solid blue line) in normalized time scale. TOr: right toe off; HSr: right heel strike. The vertical continuous line separates the swing and stance phases of gait.

The maximum orthosis torque at the ankle joint is 64 Nm (plantar flexion) for the AIS C subject and 44.2 Nm (plantar flexion) for the AIS D subject. Regarding the ankle actuation, it can be seen that the orthosis torque patterns obtained through our approach are in good agreement with the ones reported in [15], where several experiments involving healthy subjects wearing a pneumatically EMG-controlled ankle exoskeleton were performed. In the mentioned study, Kao et al. [15] showed that the total (muscles plus orthosis) ankle torque was similar to that of normal unassisted walking, and also were the knee and hip unassisted torques.

Regarding the knee actuation, the maximum extension torque during the stance phase does not change significantly between the two SCI subjects and it is about 22 Nm. During swing, the maximum torque that has to exert the orthosis to assist flexion-extension movement is 11.5 Nm (flexion) and appears at terminal swing. Although the maximum assistance torques are similar at the knee joint for both SCI subjects, it must be noted that the AIS C subject exerts a maximum muscular torque of 16.2 Nm which is lower than the one achieved by the AIS D subject, that is 22.5 Nm.

The obtained results are useful for the design of active assisting devices. The external assistance torques can be used to select proper actuators. Moreover, the chosen cost function, Eq. (7), ensures that the human-orthosis adaptation coincides with some reported experiments [15]. The obtained results must be interpreted with caution, since the muscle weakness coefficients must be evaluated in real SCI subjects. A further limitation is that the results were obtained for a pre-defined normal gait kinematics. The prediction of the resulting human-orthosis movement is a research topic that will be addressed in future publications.

#### **4. Mechanical design of an active orthosis**

The design of an active stance-control knee-ankle-foot-orthosis (A-SCKAFO) is addressed in this section. First, the technical specifications of the orthosis are outlined. Then, the main features of the mechanical design and orthosis operation are explained.

##### *4.1. Biomechanical and design specifications*

The proposed A-SCKAFO should control the flexion-extension motion of the knee joint during the swing phase and lock the knee flexion at any knee angle during the stance phase. According to the orthopedists, the actuation of the ankle motion is not essential to allow SCI subjects with AIS C and D levels to walk. The functions needed at this joint are passive dorsiflexion assistance during initial stance, to compensate for contact forces at heel landing, and during swing to avoid drop-foot or equinus gait. Fig. 6 shows the gait cycle and the specified functions of the A-SCKAFO at the knee and ankle joints.

The proposed A-SCKAFO has to include several sensors (in both the knee and ankle units) for its autonomous control. The orthosis must include plantar sensors on the insoles to detect foot-ground contact and also the period within the stance phase (initial contact, mid-stance, terminal stance). Angular sensors at both joints are also needed to detect the gait phase and they are also used as inputs of the actuation control system. These sensors will be used to switch between the stance and swing modes, this has to be done with a reaction time below 6 ms [1]. Besides the previous biomechanical and control specifications, the desired orthosis should be lightweight (a weight lower than 2.5 kg is desirable), be quiet in operation, be energetically efficient, be low cost, and support a large segment of potential users.

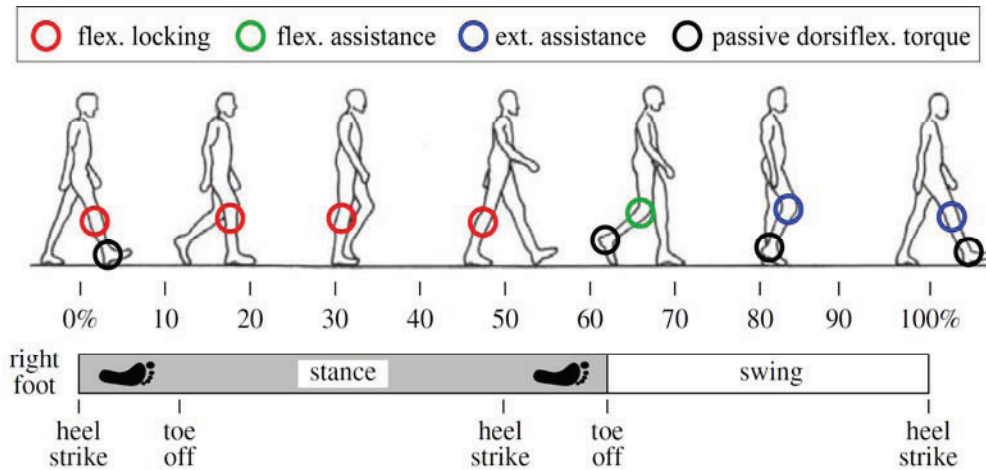


Fig. 6. Functional specifications of the active orthosis during the gait cycle. Source of the background figure: [19].

#### 4.2. Mechanical design of the ankle and knee units

The ankle unit is based on a commercial passive AFO which has been minimally modified in order to adapt an optical encoder that measures the ankle joint angle. This commercial orthosis is composed of two supporting aluminum bars which are adjusted to the shank by means of straps. In both sides of the ankle, there is a passive *klenzak* joint that applies the needed passive torque. This torque can be adjusted by modifying the initial length of a spring. The ankle unit constrains the dorsiflexion angle of the ankle to be between 0 and 20°, thus avoiding drop-foot gait. As it has been mentioned, an optical encoder has been placed on this joint to measure the ankle angle. This is an incremental encoder with a resolution of 4096 counts per turn. Each ankle unit is also equipped with a set of four contact sensors which are placed under the orthosis insole and they allow to know if contact is on the heel (initial contact), on the mid-foot (mid stance) or on the toe (terminal stance). Fig. 7 shows the CAD design of this unit.



Fig. 7. Ankle unit of the A-SCKAFO and detail of the encoder placement.

The knee unit must assist the flexion-extension motion of the knee joint during swing and lock the knee flexion at any knee angle during stance. The solution adopted for the design of this unit consists of two independent systems to assist swing and stance. The swing flexion-extension motion is assisted by means of an electrical motor, and a commercial electronically controllable locking mechanism is used to prevent knee flexion during stance. The design of the knee unit is shown in Fig. 8. The motor and the locking system are placed at the lateral and medial sides of the knee, respectively.

The commercial locking mechanism locks knee flexion by means of a pre-loaded spring that pushes a locking pawl into a toothed ring. This locking is passive and does not require energy consumption compared to other locking devices, like electrical brakes or clutches. To unlock the joint, a solenoid moves a plunger against the spring tension and the locking pawl falls out of the toothed ring. It is important to remark that in case of power or control failure, this system stays mechanically locked which is the safest situation. In this case, the patient can stand (with the knees fully extended) and walk with the aid of crutches, canes or parallel bars.

The hypothesis that subjects wearing assistive orthotic devices walk with similar joint moment patterns as in normal walking [15] allows us to select the knee actuator that assists the swing flexion-extension based on the simulations in section 3. The maximum knee torque during swing is 20 Nm and, according to simulations, the orthosis has to provide around 11.5 Nm (and 8.5 Nm the partially functional muscles). It must be pointed out that this patient-orthosis cooperation improves the patient rehabilitation. The selected motor is a “Maxon Motor EC45 flat” with a planetary gearbox with reduction 156, the gearbox is offered by the same manufacturer. The specifications of the motor plus the gearbox are shown in Table 1.

Note that according to the previous results, the actuator provides enough torque to assist the musculoskeletal system of the SCI patient during the swing phase. The actuator is equipped with an optical encoder with a resolution of 500 counts per turn (of the motor), which results in 78000 counts per turn of the gearbox axis. The encoder data serve to calculate the joint angle and angular velocity which are used as inputs of the actuation control system. It must be pointed out that linear actuators were also considered at the initial design stage. However, this option was rejected because adequate actuators in terms of volume and weight did not fulfill the required velocity specification.

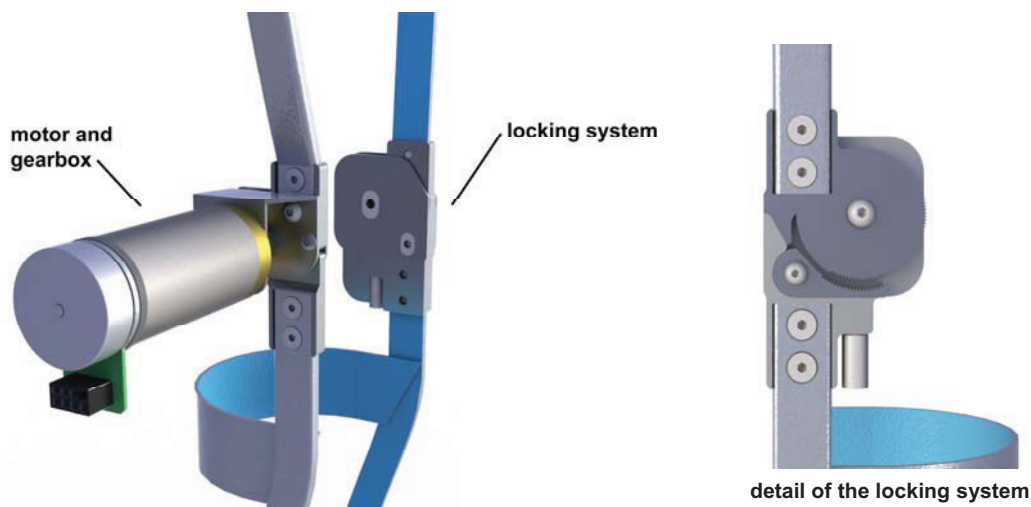


Fig. 8. Knee unit of the A-SCKAFO and detail of the locking system.

Table 1. Specifications of the motor and gearbox group at the knee unit.

Specification	Value
Nominal/Maximum torque	10.88/15 Nm
Nominal/Maximum angular velocity	33.65/43 min <sup>-1</sup>
Nominal voltage	18 V
Nominal current	3.54 A
Weight/Length	0.58 kg/87.8 mm

#### 4.3. Global design and orthosis operation

The global design of the orthosis is shown in Fig. 9. This A-SCKAFO is lightweight, the total weight of the orthosis is about 1.9 kg (motor: 0.58 kg, locking system: 0.40 kg; lateral bars and other components: 0.92 kg), and it is also energetically efficient. Moreover, the design may support a large segment of potential users, since it is adaptable to different subjects and different levels of dysfunction. This design represents a first prototype of active orthosis that will be used in a lab environment to investigate combined human-orthosis actuation and adaptation. The required sensors, the actuator and the locking system will be powered by means of an external supply unit.

The operation of the orthosis during the gait cycle is as follows: At initial stance, the plantar sensors detect contact and then the knee joint is locked; during this phase the motor does not exert any torque on the joint. During the stance phase the plantar sensors and ankle encoder data give information on the evolution of the gait cycle. Once contact is over (because the other leg has landed on the ground), the solenoid of the locking mechanism turns on to unlock the knee joint. Then, the swing phase begins and the knee actuator assists the knee flexion and then extension. The motor control during this phase will be done based on the motor and ankle encoders. After the swing phase the leg makes contact again with the ground and the new stance phase begins. At this moment, the control system is aimed at controlling the walking motion. In the future, we plan to detect and control other states such as standing or sitting down.



Fig. 9. Global mechanical design of the orthosis.

## 5. Conclusions

This work presents first a simple and efficient approach to estimate muscle forces and orthosis actuation in powered assisted walking of incomplete SCI subjects. The major contribution of the optimization approach is the integration of the contraction dynamics equations in a first step to obtain the maximum available muscle forces at each time, which ensures the physiological consistency of the results. The outputs of this approach are the efforts of the disabled subject along with the orthosis forces required to reproduce the desired normal kinetic gait patterns at joints. The weakness and atrophy of partially denervated muscles of SCI subjects have been modeled in the approach. The method is efficient from a computational point of view and provides useful results to assist the selection of actuators in the design of active orthoses. The results can also be useful to train users on how to cooperate with assistive devices to minimize power consumption. The obtained muscle-orthosis load sharing at the ankle joint presents a good correlation compared with experimental measurements reported in the literature.

Secondly, the mechanical design of an active stance-control knee-ankle-foot-orthosis is presented. The presented orthosis is aimed at assisting incomplete SCI subjects with partial denervation at the knee and ankle muscles. The ankle unit is based on a passive *klenzak* joint, and the knee unit is composed of a mechanical locking system that prevents knee flexion at stance and an electrical actuator that assists knee flexion-extension at swing. The latter actuator has been selected based on previous simulations. The prototype is equipped with the required sensors for its autonomous operation (encoders at joints and plantar sensors). The main advantages are its light weight, modularity, energy efficiency and, therefore, autonomy.

The work reported in this paper represents a first step to simulate human-orthosis interaction. Although the results are promising, several points remain to be addressed as future work. For instance, the validation of the contraction dynamics and atrophy models of denervated muscles, and the development of a forward dynamics based approach to predict the movement of the subject equipped with a specific active orthosis. In terms of orthosis design, the use of passive components, such as springs, to improve the energy efficiency of the device will be explored.

## Acknowledgements

This work is supported by the Spanish Ministry of Science and Innovation under the project DPI2009-13438-C03. The support is gratefully acknowledged.

## References

- [1] Yakimovich T, Lemaire ED, Kofman J. Engineering desing review of stance-control knee-ankle-foot orthoses. *J Rehabilitation Research & Development* 2009; **46**:257-267.
- [2] Dollar AM, Herr H. Lower extremity exoskeletons and active orthoses: challenges and state-of-the-art. *IEEE T Robotics* 2008; **24**:1-15.
- [3] Filippi P. Device for the automatic control of the articulation of the knee applicable to a prosthesis of the thigh, U.S. Patent 2 305 291, 1942.
- [4] Vukobratovic M, Hristic D, Stojiljkovic Z. Development of active anthropomorphic exoskeletons. *Medical & Biological Engineering & Computing* 1974; **12**:66-80.
- [5] Pons JL. *Wearable robots: Biomechatronic exoskeletons*. West Sussex: John Wiley & Sons, Ltd; 2008.
- [6] Hsu J, Michael J, Fisk J. *AAOS Atlas of orthoses and assistive devices*. Barcelona: Elsevier; 2009.
- [7] Romkes J, Brunner R. Comparison of a dynamic and a hinged ankle-foot orthosis by gait analysis in patients with

hemiplegic cerebral palsy. *Gait & Posture* 2002; **15**:18-24.

[8] Kaufman K, Irby S, Mathewson J, Wirta R, Sutherland D. Energy-efficient knee-ankle-foot orthosis: A case study. *J Prosthetics & Othotics* 1996; **8**:79-85.

[9] Yakimovich T, Lemaire E, Kofman J. Preliminary kinematic evaluation of a new stance-control knee-ankle-foot orthosis. *Clinical Biomechanics* 2006; **21**:1081-1089.

[10] Blaya J, Herr H. Adaptive control of a variable-impedance ankle-foot orthosis to assist drop-foot gait. *IEEE T Neural Systems & Rehabilitation Engineering* 2004; **12**: 24-31.

[11] Oymagil A, Hitt J, Sugar T, Fleeger J. Control of a regenerative braking powered ankle foot orthosis. *Proc. Int. Conf. Rehabilitation Robotics* 2007, Noordwijk, The Netherlands.

[12] Pratt J, Krupp B, Morse C, Collins S. The Roboknee: An exoskeleton for enhancing strength and endurance during walking. *Proc. IEEE Int. Conf. Robotics & Automation* 2004, New Orleans, USA.

[13] Kawamoto H, Sankai Y. Power assist system HAL-3 for gait disorder person. *Lec. Notes Comp. Science* 2002; **2398**: 19-29.

[14] Sawicki G, Ferris D. A pneumatically powered knee-ankle-foot orthosis (KAFO) with myoelectric activation and inhibition. *J NeuroEngineering & Rehabilitation* 2009; **6**:6-23.

[15] Kao PC, Lewis CL, Ferris DP. Invariant ankle moment patterns when walking with and without a robotic ankle exoskeleton, *J Biomechanics* 2010; **43**:203-209.

[16] Winter DA. *Biomechanics and motor control of human gait: normal, elderly and pathological*. 2nd ed. Waterloo: University of Waterloo Press; 1991.

[17] Zajac F. Muscle and tendon: Properties, models, scaling and applications to biomechanics and motor control. *Crit. Rev. Biomed. Eng.* 1989; **17**:359-411.

[18] Hill A. The heat of shortening and the dynamic constants of muscle. *Proc. R. Soc. London Ser. B* 1938; **126**:136-195.

[19] Ackermann M. *Dynamics and energetics of walking with prostheses*. Ph.D. thesis, University of Stuttgart; 2007.

[20] Ackermann M, Schiehlen W. Dynamic analysis of human gait disorder and metabolical cost estimation. *Arch. Appl. Mech.* 2006; **75**:569-594.

[21] Winters J. *Concepts in neuromuscular modeling, three-dimensional analysis of human movement*. Champaign: Human Kinetics Publishers; 1995.

[22] Thomas CK, Grumbles RM. Muscle atrophy after human spinal cord injury. *Biocybernetics & Biomedical Engineering* 2005; **25**:39-46.

[23] McDonald MF, Garrison MK, Schmit BD. Length-tension properties of ankle muscles in chronic human spinal cord injury. *J Biomechanics* 2005; **38**:2344-2353.

[24] Lebedowska MK, Fisk JR. Passive dynamics of the knee joint in healthy children and children affected by spastic paresis. *Clinical Biomechanics* 1999; **14**:653-660.

[25] Crowninshield R, Brand RA. A physiologically based criterion of muscle force prediction in locomotion. *J Biomechanics* 1981; **14**:793-801.

[26] Yamaguchi GT, Moran DW, Si J. A computationally efficient method for solving the redundant problem in biomechanics. *J Biomechanics* 1995; **28**:999-1005.

[27] Anderson FC, Pandy MG. Static and dynamic optimization solutions for gait are practically equivalent. *J Biomechanics* 2001; **34**:153-161.

[28] Rengifo C, Aoustin Y, Plestan F, Chevallereu C. Distribution of forces between synergistics and antagonistics muscles using an optimization criterion depending on muscle contraction behaviour. *J Biomechanical Engineering* 2010; **132**:1-11.

[29] Anderson FC, Pandy MG. Dynamic optimization of human walking. *J Biomechanical Engineering* 2001; **123**:381-390.

[30] Menegaldo LL, Fleury AT, Weber HI. A 'cheap' optimal control approach to estimate muscle forces in musculoskeletal systems. *J Biomechanics* 2006; **39**:1787-1795.

[31] Alonso J, Romero F, Pàmies-Vilà R, Lurgrís U, Font-Llagunes JM. A simple approach to estimate muscle forces and orthosis actuation in powered assisted walking of spinal cord-injured subjects. *Proc. EUROMECH Coll. 511 Biomechanics of Human Motion* 2011, Ponta Delgada, Azores, Portugal.